EARTH SURFACE PROCESSES AND LANDFORMS
Earth Surf. Process. Landforms (2015)

Published online in Wiley Online Library
(wileyonlinelibrary.com) DOI: 10.1002/esp.3729

Identification of peneplains by multi-parameter assessment of digital elevation models

Vicky L. Haider,[1]* Jan Kropáček,[2,3] István Dunkl,[1] Bianca Wagner[4] and Hilmar von Eynatten[1]
[1] Sedimentology & Environmental Geology, Geoscience Center, University of Göttingen, Göttingen, Germany
[2] Institute for Cartography, Dresden University of Technology, Dresden, Germany
[3] Institute of Geography, University of Tuebingen, Tuebingen, Germany
[4] Applied Geology, Geoscience Center, University of Göttingen, Göttingen, Germany

Received 27 September 2013; Revised 17 February 2015; Accepted 24 February 2015

*Correspondence to: Vicky L. Haider, Sedimentology & Environmental Geology, Geoscience Center, University of Göttingen, Göttingen, Germany. E-mail: vhaider@geo.uni-goettingen.de

ESPL
Earth Surface Processes and Landforms

ABSTRACT: The concept of peneplains has existed since the end of the nineteenth century. Typical peneplains are elevated geomorphological features with a low relief surface on top. They may be tilted due to tectonic activity or intersected by evolving erosion. Until now neither a standardized definition for peneplains, nor an established procedure to identify and quantify well preserved peneplains as prominent landforms existed. At present the global availability of homogeneous digital elevation models (DEMs) provides an accurate characterization of the morphology of the Earth surface. In this study a new, numerical, DEM-based fuzzy-logic approach is presented for the delineation of peneplains solely from a morphological perspective. The approach is based on a morphometric analysis of the 90-arcsec Shuttle Radar Topography Mission (SRTM) DEM. Four critical parameters are employed which are implemented within a geographic information system (GIS). The parameters for the correct and unambiguous description of a 'flat top mountain' are: (i) slope, (ii) curvature, (iii) terrain ruggedness index, and (iv) relative height. The approach was developed using a test area in the central Tibetan Plateau, which is characterized by representative and well preserved peneplains and for which additional field data were collected. In order to verify the method, peneplains were delineated in different regions with various geological settings for which potential peneplains were already described in the literature. The results from the Appalachian Mountains, Andes, Massif Central, and New Zealand confirm the robustness of the proposed approach. Copyright © 2015 John Wiley & Sons, Ltd.

KEYWORDS: geomorphology; planation; Tibetan Plateau; fuzzy logic; DEM

Introduction

Flat-top mountains have always fascinated geologists and geomorphologists. The existence of peneplains and planation as a geomorphological process is controversial, due to the lack of clear definitions and the fact that peneplains are metastable landforms. Deposition of cover sediments or uplift and erosion affect them, thus they can be found at different elevations and in different stages of decay. The term peneplain is inconsistently and cautiously used. Nevertheless, various theories about the genesis and formation of these distinctive geomorphological features have already been developed, published and discussed.

Eight different approaches are established to provide clarity regarding genesis and definition of peneplains. (1) Peneplains are generated after uplift of a young landform (Davis, 1899; Penck, 1924). (2) Peneplains develop close to sea level during periods of persistent rising of sea level (Pitman and Golovchenko, 1991). (3) They can be found at high elevation as a result of post tectonic uplift (Lamb *et al.*, 1996; Kennan *et al.*, 1997). (4) They are regarded as marine planation surfaces which have been uplifted (Garcia-Castellanos *et al.*, 2000; Landis *et al.*, 2008). (5) Peneplains are interpreted as elevated and low relief surfaces generated by glacial and peri-glacial erosion (Steer *et al.*, 2012; Hall *et al.*, 2013). (6) Piedmont aggradations of clastic sediment, derived from erosion of a high mountain range, can induce the rise of the base level around the range. This process reduces the erosion efficiency of the drainage system and results in progressive smoothing of the relief and formation of peneplains (Babault *et al.*, 2005, 2007). (7) Peneplains are the result of mantle-plume activity uplifting low-relief erosion surfaces (LeMasurier and Landis, 1996; Sheth, 2007). (8) The term peneplain is used to describe any low-relief regional-scale erosion surface without genetic connotations as suggested by Fairbridge and Finkl (1980).

Peneplains and related features termed low-relief surfaces or paleosurfaces are discussed on every continent and in many mountain belts such as the Klamath Region in California (e.g. Anderson, 1902; Aalto, 2006), the Rocky Mountains (e.g. Lindgren and Livingston, 1918; McMillan *et al.*, 2006), the Andes (e.g. Kummel, 1948; Jordan *et al.*, 1989; Hoke and Garzione, 2008; Schildgen *et al.*, 2009; Allmendinger and González, 2010), the Pyrenees (e.g. Babault *et al.*, 2005; Gunnell *et al.*, 2009), Scandinavia (e.g. Strøm, 1948; Gjessing, 1967; Lidmar-Bergström, 1999; Sturkell and Lindström, 2004; Steer *et al.*, 2012), Africa (e.g. Willis, 1933; Dixey, 1939; Coltorti *et al.*, 2007), the Himalayas (e.g. Cui *et al.*, 1997; Liu-Zeng *et al.*, 2008; van der Beek *et al.*, 2009), Australia/New Zealand (e.g. Mulcahy *et al.*, 1972; Stirling, 1991; Landis *et al.*, 2008), and Antarctica (e.g. LeMasurier and Landis, 1996).

Most peneplains were described prior to the 1960s and derive solely from field observations and topographical maps. In the last two decades, new techniques have been used to investigate peneplains such as thermochronological and geochronological tools (e.g. Jordan *et al.*, 1989; Lamb *et al.*, 1996; Gunnell *et al.*, 2009; Hetzel *et al.*, 2011; Haider *et al.*, 2013), cosmogenic nuclides (e.g Jackson *et al.*, 2002; Hetzel *et al.*, 2011; Strobl *et al.*, 2012) or geospatial data analysis (e.g. Babault *et al.*, 2005; Hoke and Garzione, 2008; Strobl *et al.*, 2010).

What is common in all the earlier mentioned studies is the observation of distinctive elevated and flat surfaces, regardless of their geological history and age. Existing definitions of peneplain are unclear and are still intensively discussed. As a consequence, it is nearly impossible to outline peneplains in a reproducible way. It is thus necessary to redefine this remarkable geomorphological structure in order to enable their unbiased identification and to foster a deeper understanding of the peneplains and the multiple possibilities for their origin.

In this study, peneplain is used as a descriptive term in contrast to the controversial definition of Davis (1899) as a genetic term. As of yet the minimum uplift of peneplains relative to their surrounding landscape is not defined. The focus lies on peneplains which are uplifted relative to their surrounding landscape by at least 100 m. The minimum specification is not a firm number so it is assumed that the likelihood decreases continuously with decreasing relative elevation towards zero.

Peneplain is referring to a distinctively elevated landform having almost plain top with a slope less than 15°. It might be slightly tilted or incised due to tectonic activity and/or advanced erosion. To a certain degree, erosion may degrade the plain surface, but no well-developed valley system or intersecting river system can be found on an intact peneplain. It is not necessarily the highest geomorphological unit in a mountain range; young tectonics or volcanism may create local heights above a peneplain.

This study focuses on peneplains from the perspective of surface morphology. The peneplains are characterized as distinct morphological units which can be defined by geomorphometric parameters, thus enabling the development of a simple and general model for the delineation of peneplains using parameters derived from digital elevation models (DEMs). For the definition of the morphological criteria, data for the central part of the Tibetan Plateau are used from where ground observations were collected. The validity and reproducibility of this geospatial approach is tested in various geological settings in different parts of the world by comparison with peneplains described in the literature.

Geological Setting and Characterization of the Peneplains North of Nam Co, Central Tibet

The central Tibetan Plateau is dominated by well-developed and preserved peneplains, this was confirmed during several field investigations (Figure 1). A peneplain identification method has been developed in this area, thus a brief description on the geology and geomorphology of the region is given.

The Tibetan Plateau is the highest and with approximately 2 million km^2 the largest plateau on Earth. More than 90% of the plateau has an elevation between 4800 m and 5400 m, and a relief of less than 1 km at a wavelength of about 100 km (Fielding *et al.*, 1994). An internal drainage system is progressively filling the intermontane basins by sediments eroded from the adjacent mountains (e.g. Métivier *et al.*, 1998; Liu-Zeng *et al.*, 2008). The highly uplifted Tibetan Plateau is the result of collision of India and Asia that generated the thickened crust (Patriat and Achache, 1984).

The study area was situated in central Tibet, along the northern boundary of the southernmost accreted terrane, the Lhasa terrane. The landscape near the lake Nam Co was studied, where elevated flat surfaces (Figures 1 and 2) with low relief are common (Clark *et al.*, 2004; Strobl *et al.*, 2010; see Figure 3). The elevation of this area is generally above 4600 m. The Nyainqentanghla mountain

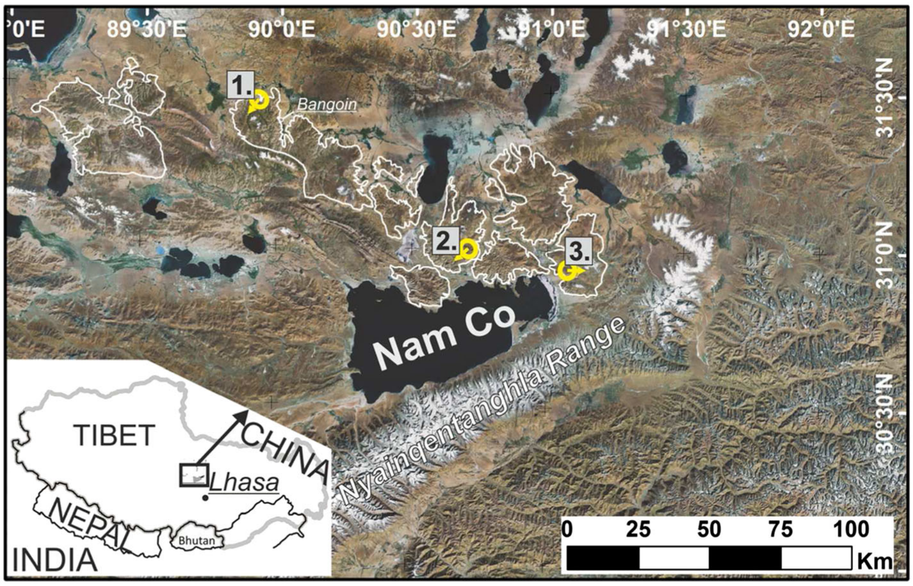

Figure 1. Landsat map showing land surface of the study area in central Tibet, the assumed peneplains (contoured with white lines north and northwest of Nam Co) and flags of taken images as examples of evidenced peneplains (yellow circles with streaks showing the directions of images of Figure 3). The assumed peneplains were determined by field observation and by the rough analysis of the available topographic maps. This figure is available in colour online at wileyonlinelibrary.com/journal/espl

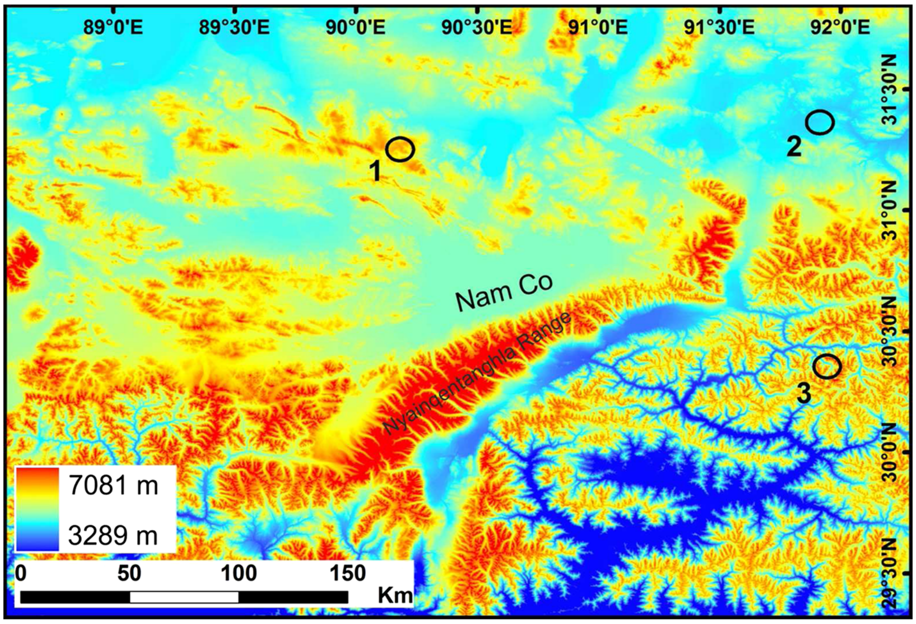

Figure 2. Shuttle Radar Topography Mission (SRTM) raster image used for modeling of the topography; the elevation of the area ranges from 3300 m to nearly 7100 m. The black circles represent areas which were sampled for detailed digital elevation model (DEM) analysis. All three circles have the same size of 10 737 data points and represent three different geomorphologic areas: circle 1, 'peneplain'; circle 2, 'average plateau'; circle 3, 'steep and dissected area'. The metadata from these circles were used for detailed statistical analysis (see Figures 5 and 8). This figure is available in colour online at wileyonlinelibrary.com/journal/espl

range borders the area to the south (Figure 2). South to southeast of this mountain range, the Tibetan Plateau is highly dissected and a well-developed river system drains the area towards the ocean. Thus the general geomorphological features of the area southeast and northwest of Nyainqentanghla range are highly different: young and steep topography in the south with a high density of river network and old, passive, and smooth topography with lakes in the north (Figure 2). The peneplains are carved mainly in a Cretaceous granitoid suite and in Jurassic metasediments (Jixiang *et al.*, 1988; Leeder *et al.*, 1988; Leier *et al.*, 2007). Peneplains west of the study area are carved also in Paleozoic metasediments (Pan *et al.*, 2004).

Materials and Methods

The Shuttle Radar Topography Mission (SRTM) DEM

The global availability of homogeneous DEMs allows a quantitative characterization of the Earth's topography. The Shuttle Radar Topography Mission (SRTM) DEM was used as a base to compute the algorithm describing potential peneplains. The SRTM provides digital topographic data of unprecedented quality across most of the Earth's surface for the international community (Farr and Kobrick, 2001). The data was acquired during an 11 days mission of the Endeavour Space Shuttle in February 2000. The single path radar interferometry at C-band recorded the topography of the Earth between latitudes 60°N and 57°S. The data is freely available on the Internet. The original SRTM DEM denoted commonly as SRTM version 3 which was assembled by Jet Propulsion Laboratory contains gaps in areas of radar shadows and low. In this study, the gap-filled version denoted as SRTM version 4 (Reuter *et al.*, 2007; Jarvis *et al.*, 2008) was used. The SRTM is available at a pixel resolution of 3 arc seconds (90 m at the Equator).

Processing of the SRTM data: the Peneplain Analyzing Tool (PAT)

The geographic information system (GIS) analyses were performed by using ArcGIS Info 9.3 and Arc Tool Spatial Analyst. As spatial reference system, UTM projection and WGS84 datum were used. Depending on the size of analyzed area, several image tiles were assembled into a single mosaic. In the following step the basin-like artifacts were filled-up by using a standard procedure of ArcGIS where the tool iterates until all sinks are filled (Tarboton *et al.*, 1991). This procedure is necessary to enable an automatic and representative identification of drainage structure in the following step (Figure 4A). The pixel resolution of 3 arc seconds persists through the complete modeling procedure.

The new Peneplain Analyzing Tool (PAT) based on derivation of multi-assessment parameters was implemented in an interactive environment of ArcGIS Modelbuilder. Figure 4A displays a schematic overview of the structure of PAT. The raster analysis was always performed by using the smallest floating window, namely three-by-three pixels to keep the high resolution of the original DEM through the complete modeling procedure. Only at the focal statistics in the last step of the modeling procedure the floating window size is expanded to 55 by 55 pixels. This last step was established to obtain compact areas of possible peneplains in the final outcome. The used cell size of about 495 m × 495 m delivers the best output visualizing possible peneplains and emphasizes their boundaries. The performance with higher resolution data are too detailed for our approach. Nevertheless, this setting can be modified depending on the purpose.

Characterization of peneplains by geomorphometric parameters

We hypothesize that peneplains can be characterized by a set of parameters describing the morphology of a flat-top

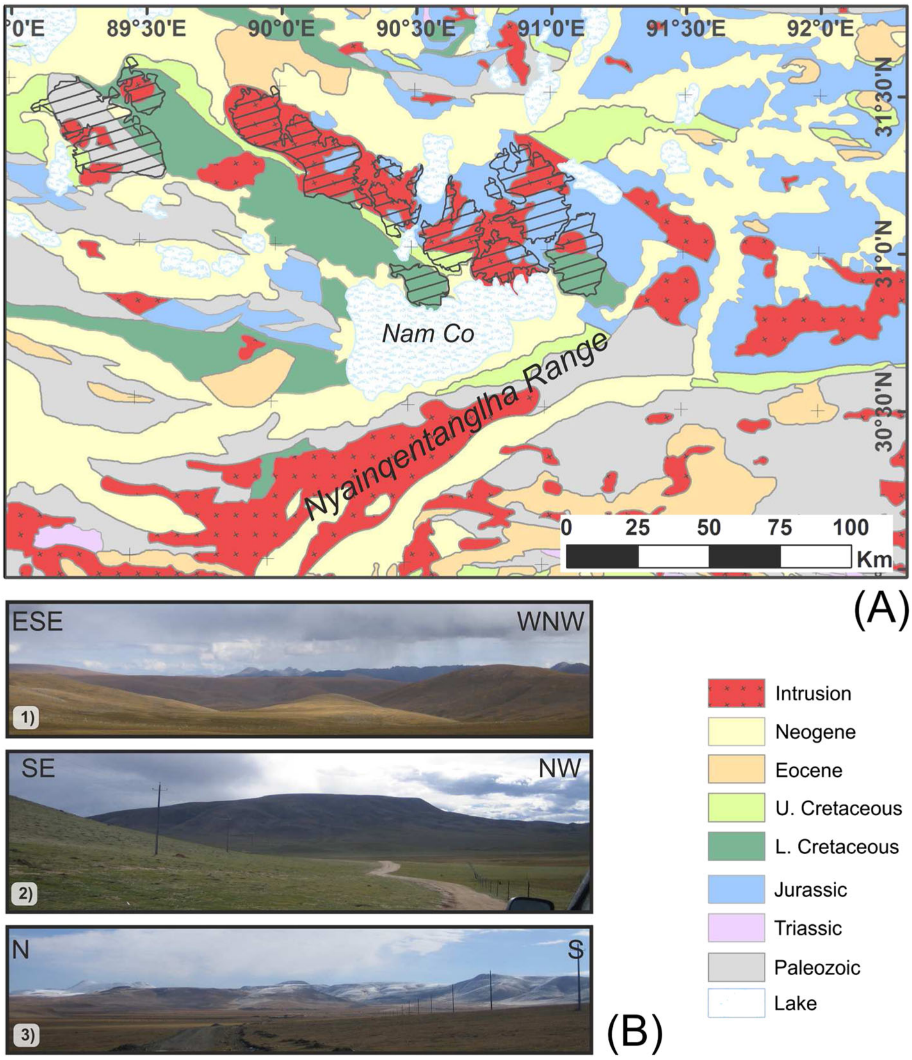

Figure 3. (A) Assumed peneplains (hatched areas) plotted on the geological map of the study area (Pan *et al.*, 2004). The local geology does not have an impact on the development of peneplains; they are formed both in granitoids and in (meta-) sedimentary formations. (B) Landscape photographs of peneplains from three different areas of the field; see locations in Figure 1. Images 1 and 2 display peneplains carved into Cretaceous granitoids while image 3 shows peneplains formed in Cretaceous volcano-sedimentary sequence. This figure is available in colour online at wileyonlinelibrary.com/journal/espl

mountain. These parameters would allow us to identify peneplains in an unbiased way regardless of their genesis, geology, and geographic location. For identification of planation surfaces, various morphological parameters that can be derived from the rough DEM data were tested. A systematic search was performed for suitable parameters describing the geomorphological features to constrain peneplain morphology. Finally, four parameters were selected: (1) slope inclination, (2) curvature, (3) terrain ruggedness index (TRI), and (4) relative height.

All four parameters were collected on a pixel-by-pixel basis in a floating window. None of these parameters alone can describe the morphology and identity a 'flat-top' mountain. For a joint evaluation, the four parameters have to be normalized and they should be given a weight. This was accomplished using a fuzzy logic procedure (e.g. Zadeh, 1968; Santos, 1970; Biacino and Gerla, 2002). Therefore, fuzzy logic was used in order to convert the magnitude of the parameters to membership degree that a pixel under consideration belongs to a peneplain. Fuzzy logic allows us to define the peneplain threshold class value by a smooth transition rather than by a hard threshold which better respect the character of the peneplain definition.

To set up the parameters, which characterize peneplains in a complete and unbiased manner, three representative test areas from basically different landscapes were analyzed. Each area contains 10 737 pixels sampled in a circle that is placed on a (i) well-developed peneplain, (ii) on a typical plateau and (iii) on an area characterized by rugged mountainous relief and rapid erosion – called later a 'steep and dissected area' (Figure 2). Density scatterplots show the different behavior of the datasets from the different test areas (Figure 5). While the dataset of 'steep and dissected area' scatters nearly over the whole diagram, the datasets of 'peneplain' and 'average plateau' occupy small areas on the plots. Scatterplots of curvature versus relative height show the best discrimination between 'peneplain' and 'average plateau'. With fuzzy logic it is possible to capture all data belonging to peneplains and to exclude all other data points. Fuzzy logic weights the values of each parameter individually and converts the different magnitudes into likelihood (membership degree) (Figure 4B).

Implementation of the criteria in the GIS environment

Slope (sl)

Slope inclination results as a maximum rate of change between each cell and its eight neighbor cells at the DEM. The slope inclination for the model is calculated with standard tools

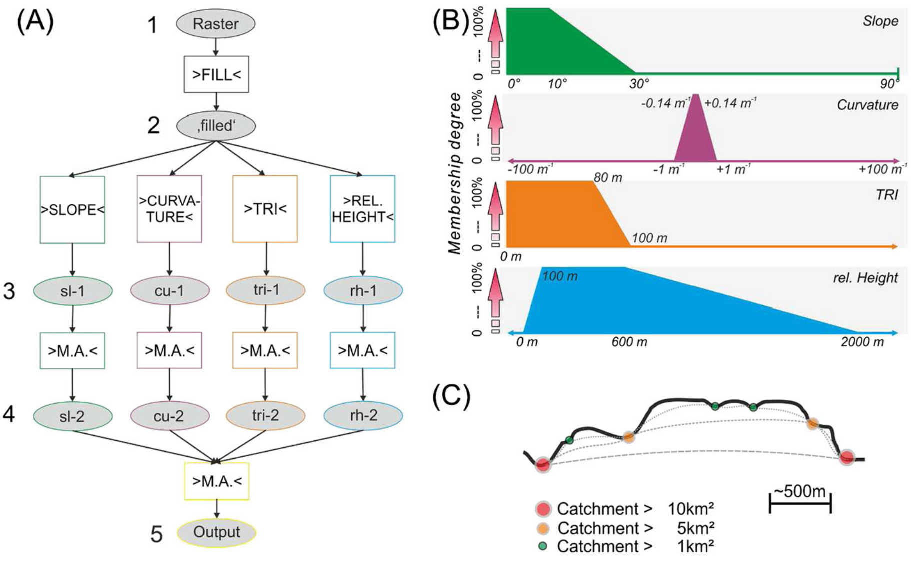

Figure 4. (A) Schematic workflow chart developed for the identification of peneplains. Step 1, input; step 2, closure of the erroneous small pixel holes and gaps in raster; step 3, meta output of four calculation strings (slope, curvature, terrain ruggedness index [TRI], and relative height); step 4, converting meta output to appropriate raster set with fuzzy logic method and map algebra (MA); step 5, output of final map after multiplication of all four meta raster with map algebra. (B) Fuzzy logic chart of each single calculation string. The *Y*-axis represents 'membership degree' in percentage; the maximum value of each curve is 100%, the minimum value is zero. (C) Schematic sketch outlining the effect of different threshold settings of the valley system for calculating catchments and thus calculating erosional base level (gray dashed lines). While interpolation between catchment of 10 km^2 cuts huge amount of information off, interpolation between catchment 1 km^2 has higher resolution. This figure is available in colour online at wileyonlinelibrary.com/journal/espl

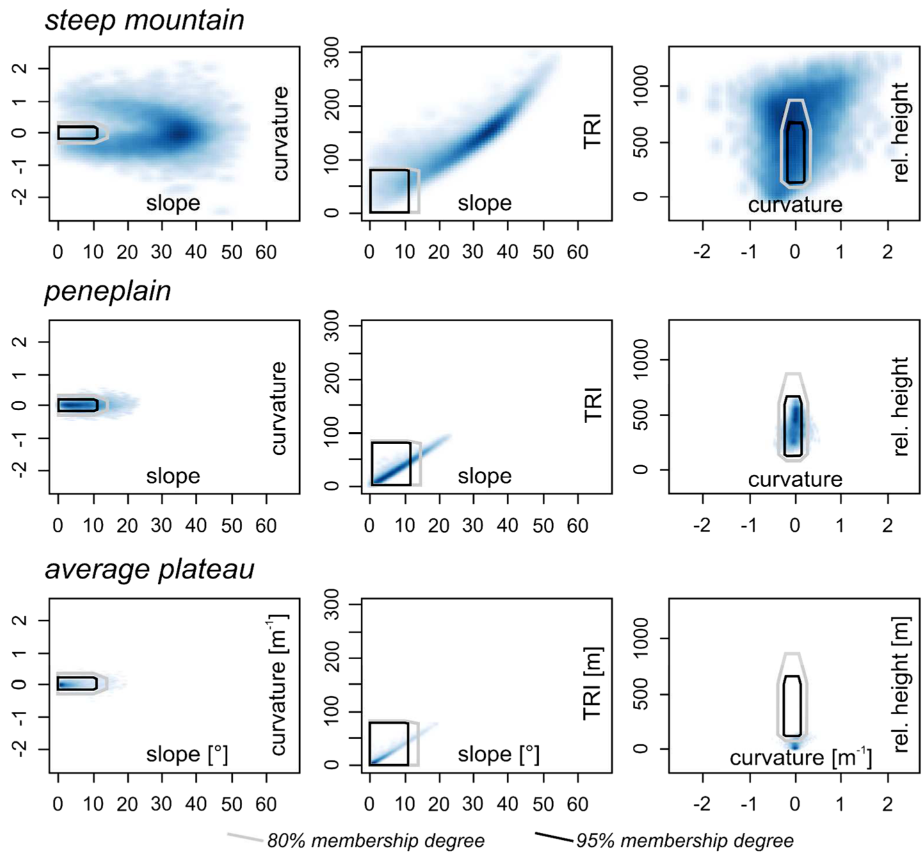

Figure 5. Density scatterplots from the metadata of three different areas marked in Figure 2. Each plot was generated from 10 737 DEM pixels of the selected areas. Scatterplots of the upper row concerns the 'steep and dissected area', while the middle row represent results of 'peneplain' and the lower row apply to 'average plateau'. Gray and black shapes in the plots outline the 'high likelihood parameter field' used at fuzzy logic (see text for explanation). Data points plotting in the gray shapes have a membership degree of > 80%, while data points inside the black rimed 'high likelihood parameter field' hold a membership degree of > 95%. This figure is available in colour online at wileyonlinelibrary.com/journal/espl

(Burrough and McDonell, 1998). Nevertheless, slope solely is not sufficient for detection of potential peneplains because lakes and other flat areas, as e.g. alluvial basins, also have low slope.

The slope is naturally limited to a value between 0° and 90°. For the identification of peneplains, the primarily the low angle slope data are relevant. However, peneplains can be tilted by tectonic activity. Therefore, it is problematic to set an explicit boundary between 'still being a peneplain' and 'definitely not a peneplain'. With increasing slope the likelihood of a possible peneplain decreases. Peneplains with a slope up to 10° are highly possible and becoming continuously implausible towards slope > 30° (Figure 5). Such situations are well-posed for the fuzzy logic approach. If an elevated planar surface is tilted more than 15°, it is clearly not matching any criterion considered until now in the related geomorphological literature at the definition of a peneplain and thus such surface can be disregarded.

Thus, the fuzzy logic criteria is set as follows: > 30° are set to 0%; 0°–10° are set 100% and values from 10° to 30° change continuously from 100 to 0% (Figure 4B). With this fuzzy logic criteria the likelihood of a peneplain with a slope of 14° is 80%.

Curvature (cu)

Curvature for any direction is the second derivate of the surface or in other words, a function 'slope of a slope' described by Zevenbergen and Thorne (1987) and Peckham *et al.* (2011). Profile and plan curvature can be calculated which are related to the concavity (negative values) and convexity (positive values) of the surface (Olaya, 2009). Zero value describes a plain surface independently of inclination. Curvature is broadly used in terrain analysis in hydrology and soil erosion studies (Zevenbergen and Thorne, 1987; Olaya, 2009; Peckham *et al.*, 2011; Hurst *et al.*, 2013). As potential parameter for PAT, curvature distinguishes planar surfaces and excludes zones along mountain crests which cannot be distinguished by the parameter slope. Curvature correlates to slope in flat areas (~0 m^{-1} versus ~0° slope) while the characteristics can diverge in steep realms (Figure 5). The excluded areas are generally small and easy to distinguish from potential peneplains in the final model.

Curvature with values near zero can characterize potential peneplains. The curvature can be high only at the rim of the peneplain, along the transition zone towards rugged, eroding areas. For the calculation of curvature, the standard tool implemented in ArcGIS involving combined plan and profile curvature is used, which calculates an inverse curvature range between –100 and +100 m^{-1}.

The fuzzy logic criteria: ranges < –1.0 and > 1.0 m^{-1} are set to 0%; ranges < –0.14 and > 0.14 m^{-1} are set 100% and ranges –0.14 to –1.0 m^{-1} and 0.14 to 1.0 m^{-1} respectively change linearly from 100 to 0% (Figure 4B).

Terrain ruggedness index (TRI)

The TRI is the summed change in elevation between a grid cell and its eight neighbor grid cells (Riley *et al.*, 1999). It was developed to characterize surface ruggedness and quantify topographic heterogeneity such as steep and dissected area and undulating surface. The following formula is adopted for calculation of the TRI:

$$TRI = \sqrt{x + 9v^2 - 2vs}$$

where x the focal sum of the squared DEM cells ($[DEM]^2$), v for focal value and s for focal sum in the floating window 3 by 3 raster cells.

Zones of active and rapid erosion are typically localized along the decaying margins of the peneplains and the internal, flat part remain intact for a longer time period, thus these areas are characterized by low TRI values. Together with curvature and slope, TRI values exclude areas with surface undulations. Both, curvature and TRI behave similar in plain realms with values ranging near zero. The more rugged the topographical surface becomes, the higher is the variance of TRI and curvature value due to increasing TRI independently of the curvature (Figure 5).

The parameter TRI provides an opportunity to distinguish between rough geomorphology (typically the result young incision) from a flat or hilly and nearly featureless surface. While a high TRI value is characteristic to mountainous areas, flat landscapes yield low TRI values. The calculated TRI value can vary from zero to several hundreds of meters. The threshold for values involving peneplains is set empirically by testing different value range and analyzing the scatterplots of datasets. See discussion of this parameter later and in Figure 5.

The fuzzy logic criteria: Values between 0 m and 80 m are accepted to indicate potential peneplains with a likelihood of

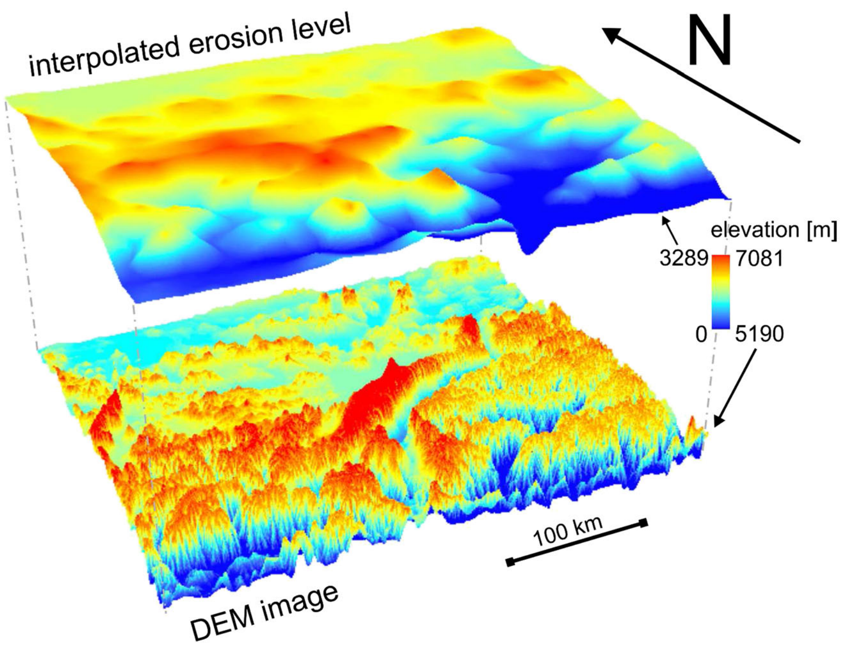

Figure 6. The relative height results from subtraction of interpolated erosional base level from the DEM. For better visualization both layers are 20 times vertically exaggerated. The result from this specific example, and more explanation, is given in Figure 7C. This figure is available in colour online at wileyonlinelibrary.com/journal/espl

100 %. While values higher than 100 m are set to 0%, the membership degree gradually decreases from 100% to 0% between 80 m and 100 m (Figure 4B).

Relative height (rh)

Since the focus lies on peneplains which are detectable elevated relative to their surrounding landscape, a suitable parameter is needed to describe this relative height. Therefore, this ‘relative height’ can be defined as the elevation above the local erosional base level represented by main branches of the drainage system. The erosional base level was obtained by interpolation of elevation data between the branches which were detected automatically, as streams with high flow accumulation. Here, the standard hydrological tools in Spatial Analyst were used.

The purpose to introduce the ‘relative height’ into our model is primarily to eliminate plain surfaces near local erosional base level to delimit potential peneplains.

The first step in the calculation of the relative height is the determination of flow direction for each raster cell. Based on this new dataset the catchment area can be determined for each cell by the summation of the upstream cells. In other words, it is the catchment area, which drains to the cell under examination. The next step is the calculation of a drainage system (valley network) applying a threshold for the catchment area. The erosional base level used in the model is a surface generated by interpolation of the afore calculated drainage systems (Figure 6). It is obvious that the considered drainage network highly influences the erosional base level. If too detailed a drainage network is used for interpolation, then the erosional base level would ‘follow’ the surface and thus the relative height would be low. If the interpolation between the branches of the drainage system is too rough (i.e. only tributaries considered with large catchment area), then the interpolated erosional base level would remain at low elevation, resulting in a relative height that allows detecting large and complex peneplain areas (Figure 4C).

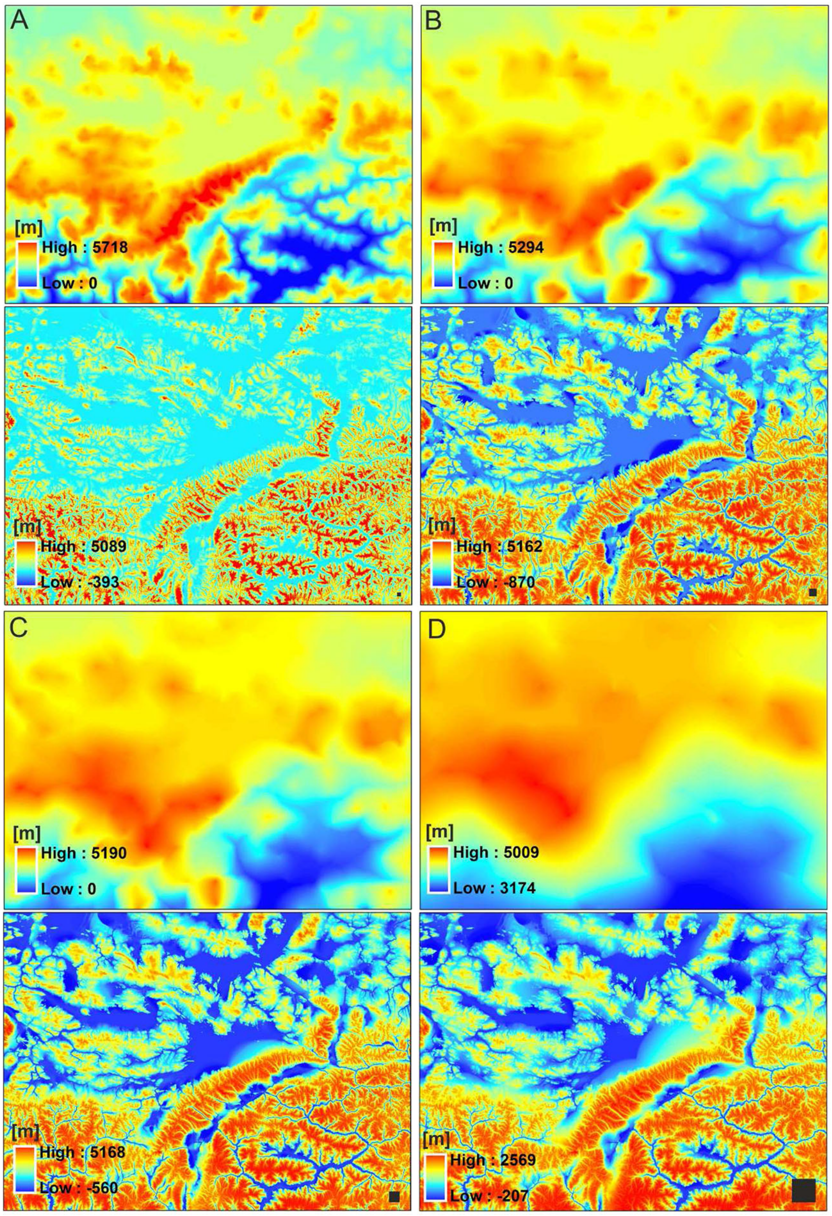

Figure 7. Series of images show the impact of the calculated erosional base level on the relative height (the area is shown in Figure 1). The upper image of each set shows the erosional base level resulted by interpolation between rivers with different threshold settings. The lower image of each set shows the relative height calculated by subtraction of the interpolated erosional base level from the original SRTM digital elevation raster (Figure 1). The black square at the bottom right corner symbolizes the size of catchment area (A = 1000, B = 5000, C = 10 000, D = 50 000 DEM pixels) used as threshold at the determination of the drainage system for the calculation of erosional base level. This figure is available in colour online at wileyonlinelibrary.com/journal/espl

The resolution of the drainage system defines the size of valleys that will be considered. The more developed the drainage system, the higher is the number of the cells in the catchment area related to the investigated cell. By using different cell numbers of the DEM e.g. 1000, 5000, 10 000 and 50 000 the corresponding catchment areas are *c.* 8.1, 40.5, 81, and 405 km^2. These cell numbers were used for testing the sensitivity; a catchment area threshold set to 5000 DEM pixels is too detailed to interpolate representative erosional base level, while using 50 000 DEM pixels removes too much information and smoothes the erosional base level too much (Figure 7). The threshold of 10 000 pixels resulted in the most applicable erosional base level in our test runs, thus this empirically determined the value of the catchment area used for interpolation.

As defined earlier, the relative height is the vertical difference between the landscape surface and the envelope of the erosional base level calculated according to the considered valley bottoms of the studied area. Relative height allows distinguishing peneplains that are elevated above their surroundings, e.g. from other flat landscapes like lakes, swamps, sedimentary basins, and low-angle alluvial fans, because these are always at the erosional base level or only slightly above it. The relative height value can range between zero and the maximum relief value of the studied area. After evaluating different settings empirically, a threshold is set as follows: between 100 and 600 m is set to 100%; less than zero and higher then 2000 m is set to 0%; between 100 and 0 m and between 600 and 2000 m the membership degree change linearly from 100 to 0% (Figure 4B). This parameter value practically excludes geomorphological domains only slightly elevated above their surroundings. The reason for selecting such high threshold values derives from the geomorphology of our primary study area. In central Tibet the young, brittle, extensional tectonics generated well developed 'horst-and-graben' landscape, where the elevated peneplains are situated typically a few hundreds of meters above the alluvial filled basin areas. The PAT system is flexible and allows for the threshold for fuzzy logic to be set for lower values, according to the intensity of young erosional or tectonic differentiation of the surface.

Evaluation of the test areas using the fuzzy logic thresholds

According to the fuzzy logic thresholds the areas of > 80% and > 95% likelihood are outlined on the different projection planes represented by the scatterplots of Figure 5. While most of the data of the 'peneplain' test area fit into the high membership degree parameter field of all scatterplots, the relative height cut out the data of 'average plateau'. Most of the dataset within the selection of 'steep and dissected area' fall outside of the high membership degree parameter field (similarly to the observation of Roering *et al.*, 2005).

After applying fuzzy logic and multiplication of all four parameters, the analyzed data from the three test areas were plotted as bar charts (Figure 8). Figure 8 shows the membership degree of the three, geomorphologicaly different test areas belonging to a peneplain. The data of 'steep and dissected area' spreads over the whole membership degree scale, but more than 95% have a membership degree less than 60% and the majority of the data have a membership degree between 0 and 20%. The data of 'average plateau' has a membership degree lower than 50% with the highest frequency at 10%. More than 95% of data of 'peneplain' have a higher membership degree than 80% and the majority of the data is even above 95%. This matching of peneplain data and the obvious misfit of the points derived from the test areas of 'steep and dissected area' and 'average plateau' emphasize the robustness of the earlier outlined DEM-based automatic identification scheme of peneplains.

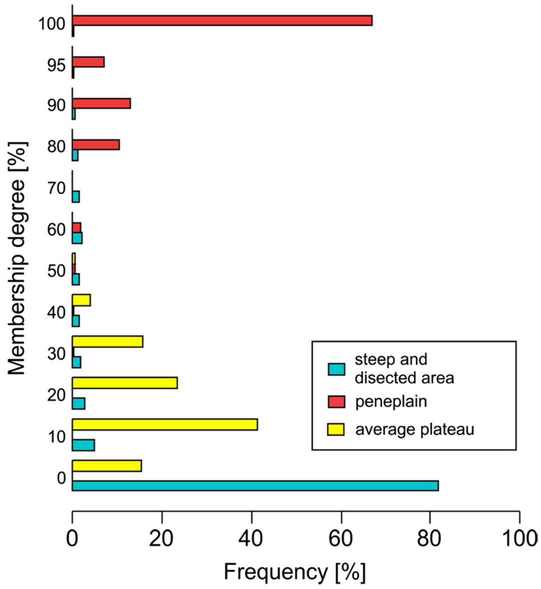

Figure 8. Bar charts showing the membership degree distribution of the pixels of the selected circular test areas (see their position in Figure 2). The membership degree of the peneplain is calculated by the fuzzy logic multiplication of the four parameters (discussed in the text). The high score of the 'peneplain' test area and the very low score of the 'high mountains' test area is obvious. This figure is available in colour online at wileyonlinelibrary.com/journal/espl

Results

Peneplains identified in Nam Co area in central Tibet

Beyond the selected test areas (Figure 2), the peneplain identification procedure was performed on the entire Nam Co area, where data across three field seasons were collected and geomorphological observations were gathered. Neither the single parameters, (Figure 9, upper panels), nor the fuzzy logic applied to the single parameters (Figure 9, lower panels) identify peneplains optimally. Figure 10 presents the integration of the four parameters in a single map. The final result is a map that shows the likelihood expressed as membership degree that a given area can be considered as a peneplain. Focusing on calculated peneplains with a membership degree of > 80% in the study area, they coincide with observed peneplains in the field (see inset in Figure 10). The fuzzy logic based map of peneplains shows occurrence of peneplains not only north of Nam Co, but also in the Amdo Basement (Figure 10, right top corner). Along the Nyainqentanghla range and south of it no significant areas of peneplain character could be detected except a few small spots. In the inset image of Figure 10 the known peneplains of Nam Co are shown in detail and are compared to the rough contour of the previously assumed extent of the peneplains. The latter coincides well with the automatically identified peneplains.

Verification of PAT on peneplains identified and mapped in previous studies by various authors

The proposed approach was tested at four independent areas located in the Andes, Appalachian Mountains, Pyrenees, and southern New Zealand (Figures 11 and 12) where peneplains have already been described and discussed by different authors. The same parameter settings were used for modeling of these areas that were applied in the Tibetan Plateau.

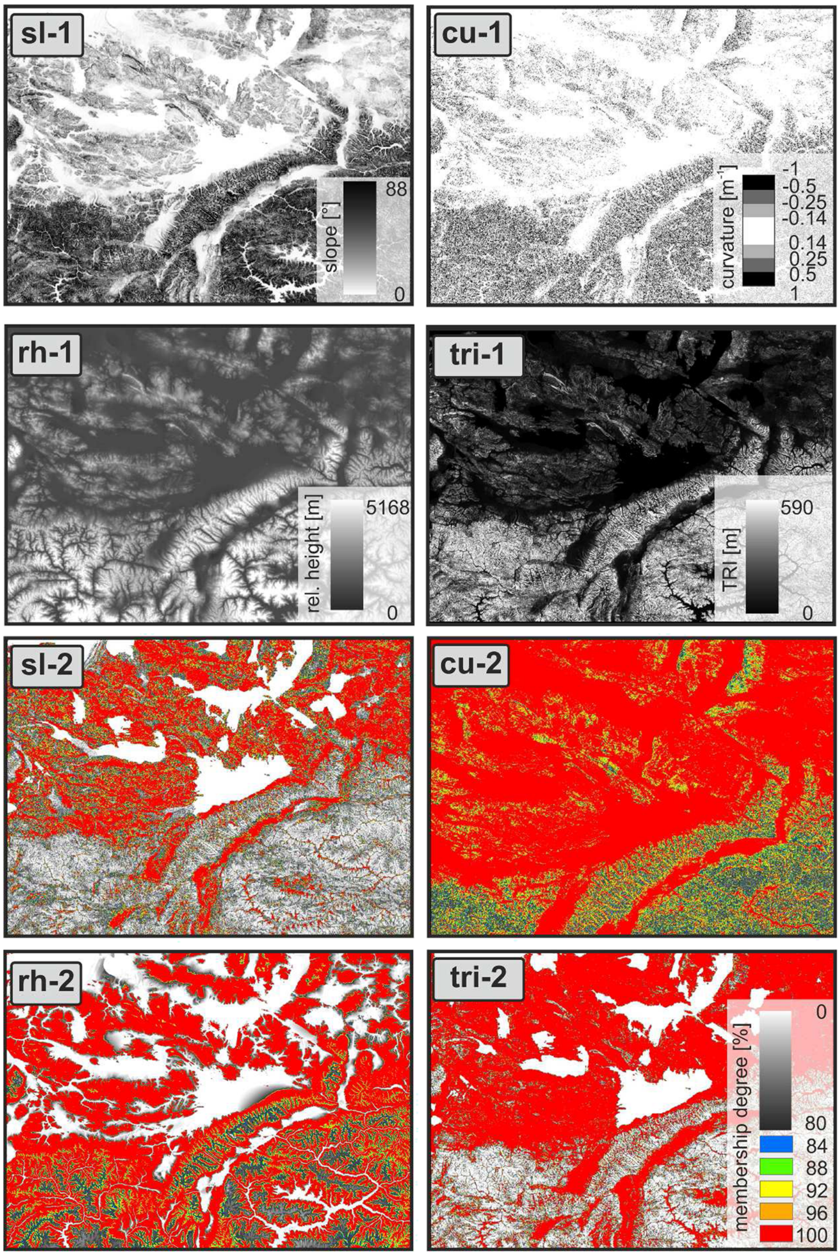

Figure 9. The upper panel shows the four parameters: slope (sl), curvature (cu), relative height (rh), and terrain ruggedness index (TRI) calculated for the Nam Co area (see topography of the area and geological map in Figures 2 and 3). The colored maps in the lower panel present the membership degree after fuzzy logic conversion (only membership degree above 80% are colored, the lower values remained gray-scaled). This figure is available in colour online at wileyonlinelibrary.com/journal/espl

Andes

In the central Andes in the region of the Altiplano numerous publications mention peneplains or elevated planation surfaces or paleosurfaces. In the northern area peneplains were described by e.g. Kummel (1948) and Campbell *et al.* (2006), while examples in the south are given by e.g. Jordan *et al.* (1989) and Hoke and Garzione (2008). In the central Andes in northern Chile and Bolivia, Lamb *et al.* (1996) mentioned – among others – peneplains in the Eastern Cordillera around Juan de Oro Basin. Kennan *et al.* (1997) also studied the Eastern Cordillera and used for the observed geomorphology the expression 'highly elevated plain surface'. Hoke *et al.* (2007) mentioned pediments and paleosurfaces. Further south in Sierras Pampeanas Jordan *et al.* (1989) studied peneplains from a thermochronological point of view. Galli-Olivier (1967) and Muñoz *et al.* (2008) investigated peneplains in the Tarapacá Region (northern Chile), whereas Galli-Olivier (1967) interpreted the observed geomorphology as pediplain. Allmendinger and González (2010) started the modern deformation cycle with a long period of erosion that culminated in a regional surface as the Tarapacá peneplain.

PAT detects peneplains along the coast and also in several spots in the highly elevated parts of the orogen (Figure 11A). Peneplains along the coast outline the ramp-like piedmont areas between the Western Andean Escarpment and the Coastal Cordillera in northern Chile and southern Peru (e.g. Wörner *et al.*, 2002; Schildgen *et al.*, 2009). Notably, peneplains on the Altiplano typically scatter around the basins. A well-studied peneplain is the Tarapacá Peneplain between Altiplano and Atacama Desert (Figure 11A), which is also clearly identified by PAT. The intermontane basins and big lakes as Lake Titicaca are correctly classified as non-peneplain although they share many characteristics (slope, ruggedness and curvature) with peneplains. However, the relative height is low in these geomorphological domains, thus PAT classifies the intermontane basins in the Altiplano or in the Atacama area with a very low membership degree (around 0%).

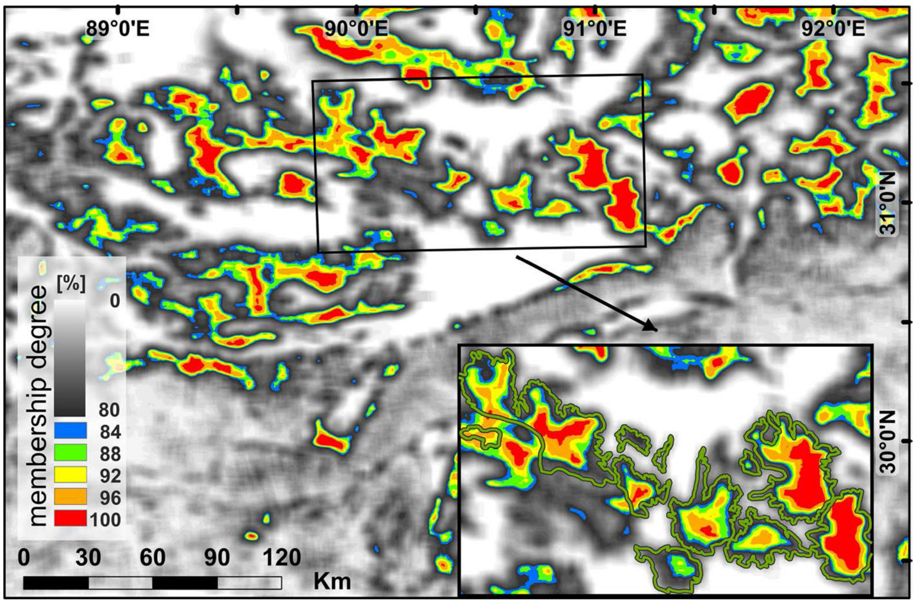

Figure 10. Map of the peneplains of the Nam Co area identified by the fuzzy logic integration of the four parameters (presented individually in Figure 10). Areas with a higher membership degree than 80% are colored while the others are kept in shades of gray. The main peneplain area shown in the rectangle is enlarged in the inset (lower right). The inset shows also the preliminary contour of the peneplain (green line) according to our field observations and the evaluation of the available topographic information. This figure is available in colour online at wileyonlinelibrary.com/journal/espl

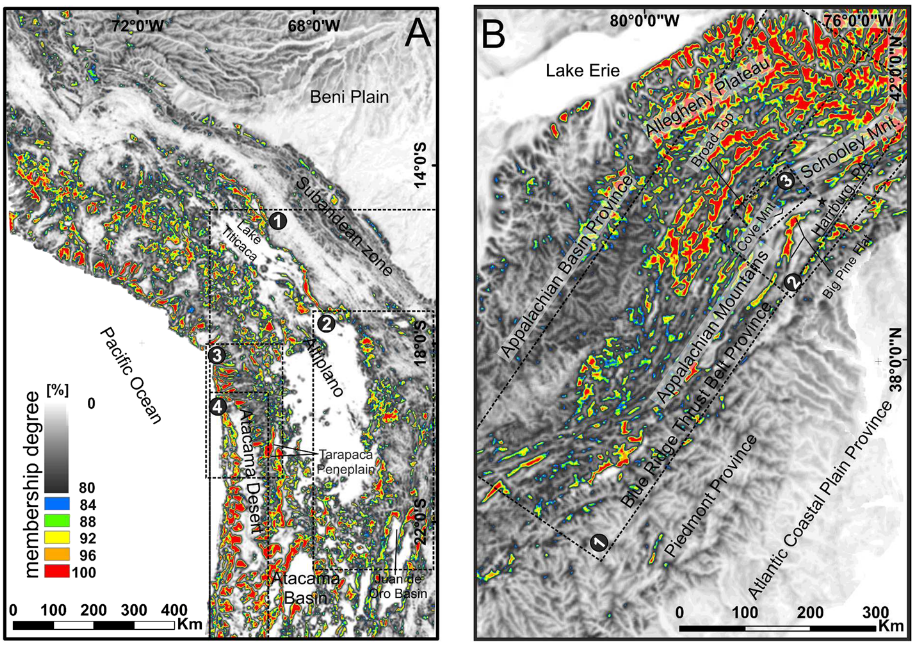

Figure 11. Peneplains and their membership degree identified by the PAT method in the Andes (A) and in the Appalachian Mountains (B). Rectangles with dotted lines allocate the formerly studied peneplain-bearing areas by different authors. Andes: ❶ (Lamb *et al.*, 1996; Kennan *et al.*, 1997; Muñoz *et al.*, 2008; Allmendinger and González, 2010), ❷, ❸, and ❹. Appalachian Mountains: ❶ (Davis, 1899; Stose, 1940; Bethune, 1948; White, 2009), ❷ and ❸. This figure is available in colour online at wileyonlinelibrary.com/journal/espl

Appalachian Mountains

William Davis (1899, 1902) intensely studied the morphology of Appalachian Mountains before introducing the term peneplain for the first time. He investigated his *Geographical Cycle* peneplains in the whole Appalachian Mountains but focused mainly on the northern part. Therefore, this area was selected to test our new model (Figure 11B). The Appalachian Mountains cross the eastern part of the United States from north-northeast (NNE) to south-southwest (SSW). Allegheny Mountain forms the north-western part of the Appalachian Mountains bordering to the Appalachian Basin Province and the Allegheny Plateau. In this area many studies were performed about peneplains in the first half of the twentieth century (e.g. Fridley and Nölting, 1931; Cole, 1934; Smith, 1935). The Schooley Mountains are found in the north-eastern part of the Appalachian Mountains. Peneplains from this area were described by many studies (Stose, 1940, and references cited therein; Bethune, 1948; Hack, 1975; Sevon *et al.*, 1983; White, 2009). Bethune (1948) did not study peneplains actively but accepted the peneplains as part of the Schooley Mountains and part of the Davisian Cycle. He proposed the hypothesis that the Appalachian drainage was substantially reorganized at the time of uplift of the 'Schooley peneplain'. Hack (1975) evaluated the theory of Davis (1899) in the Appalachian

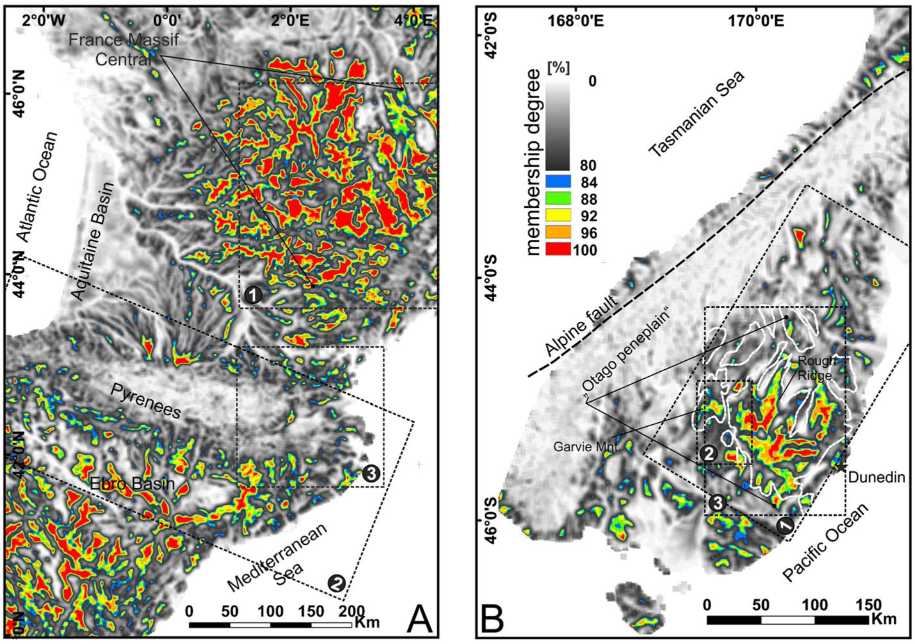

Figure 12. Peneplains and their membership degree identified by the PAT method in north-eastern Iberia and in the Massif Central (A), and in the southern part of New Zealand (B). White lines highlight the peneplains mapped by Jackson *et al.* (1996). Rectangles with dotted lines show the peneplains discussed by other authors. North-eastern Iberia and Massif Central in France: ❶ (Simon-Coinçon *et al.*, 1997; Babault *et al.*, 2005; Gunnell *et al.*, 2009), ❷ and ❸. New Zealand: ❶ (Adams, 1980; Stirling, 1991; Jackson *et al.*, 1996), ❷ and ❸. This figure is available in colour online at wileyonlinelibrary.com/journal/espl

Mountains around Harrburg and studied the principle of dynamic equilibrium in multiple erosion cycles forming landscape features. Hack (1975) challenges the peneplain concept as genetic expression and accepts it as definition of true erosion in a broader understanding of Earth surface processes.

PAT was used to identify the peneplains in this well studied part of the Appalachian Mountains. Several peneplains especially on the north-western rim of the Appalachian Mountains and some near the border to the Blue Ridge Thrust Belt Province in the east were detected. PAT spots the highest density of peneplains in the northern part of Allegheny Mountain. PAT recognizes the peneplains that are outlined in the works of Stose (1940), Hack (1975) and White (2009) with a minimum relative elevation of 80 m in this area (see Figure 11B, rectangle number 3). Nearly leveled peneplains with an elevation lower than 80 m are not considered by PAT in first instance using the default setting.

Northeast Iberia and the Massif Central

For identification of peneplains an area in western Europe (Figure 12A) was selected because of (i) the controversy discussions on the development of the peneplains in the Pyrenees (Babault *et al.*, 2005, 2007; Gunnell *et al.* 2009; Sinclair *et al.* 2009), and (ii) the presence of well developed peneplains in the Massif Central, France (e.g. Simon-Coinçon *et al.* 1997).

The Massif Central forms an exhumed part of the European Variscan basement. After erosion to a peneplain and a marine transgression the area was reactivated during Alpine orogeny (Zeyen *et al.*, 1997). Baulig (1957) and Simon-Coinçon *et al.* (1997) discussed the occurrence of peneplains as paleosurface from Tertiary time. Beneath the Massif Central mantle plume activity was detected (Granet *et al.* 1995), which is considered responsible for the continuous uplift of the Massif Central. Our PAT analysis detects several potential peneplains in the area of the Massif Central (Figure 12A). Further potential peneplains were detected south of the Ebro basin.

In the Pyrenees peneplains were described by DeSitter (1952), Babault *et al.* (2005), Gunnell *et al.* (2009), and Sinclair *et al.* (2009). Babault *et al.* (2005) considered peneplanation in the highly elevated areas of the Pyrenees as a result of long-term erosion processes that smooth relief even at high elevation. Gunnell *et al.* (2009, p.1) related the highly elevated flat topography in the eastern Pyrenees to 'the resurrection of a mountain belt which prior to the ~12 Ma was a low-relief landscape, or peneplain, beveling eroded stumps of the Pyrenean compressional orogen'.

Our modeling using PAT could not detect proper developed peneplains in the Pyrenees. It identifies only some minor areas with a membership degree mostly less than 92%. Those geomorphological domains can be eventually interpreted as remnants of old peneplains.

Southern New Zealand

Peneplains in the south of New Zealand belong to the most studied peneplains worldwide. Several authors described and investigated peneplains directly or indirectly in the southern part of New Zealand in the region of Otago (e.g. Coombs *et al.*, 1960; Adams, 1980; Stirling, 1991; Jackson *et al.*, 1996; Markley and Norris, 1999; Jackson *et al.*, 2002; Landis *et al.*, 2008). According to Coombs *et al.* (1960) and Stirling (1991) the peneplains developed in the Late Tertiary, which corresponds to a low-relief surface in central Otago. The authors examined also the degree to which the peneplain has been modified by non-tectonic processes. Adams (1980) identified and outlined the Otago peneplain as still a visible geomorphological feature. Jackson *et al.* (1996) mapped peneplains in southern New Zealand.

Very distinctive areas are recognized by PAT that were already classified as peneplains (Figure 12B). The calculated peneplains coincide with the roughly outlined peneplains after Adams (1980). PAT reproduces very good area-wide peneplains as mapped by Jackson *et al.* (1996) (Figures 12B). Peneplains described at Rough Ridge (Jackson *et al.*, 2002) and Garvie Mountains (Stirling, 1991) are clearly recognizable in the generated peneplain-likelihood map.

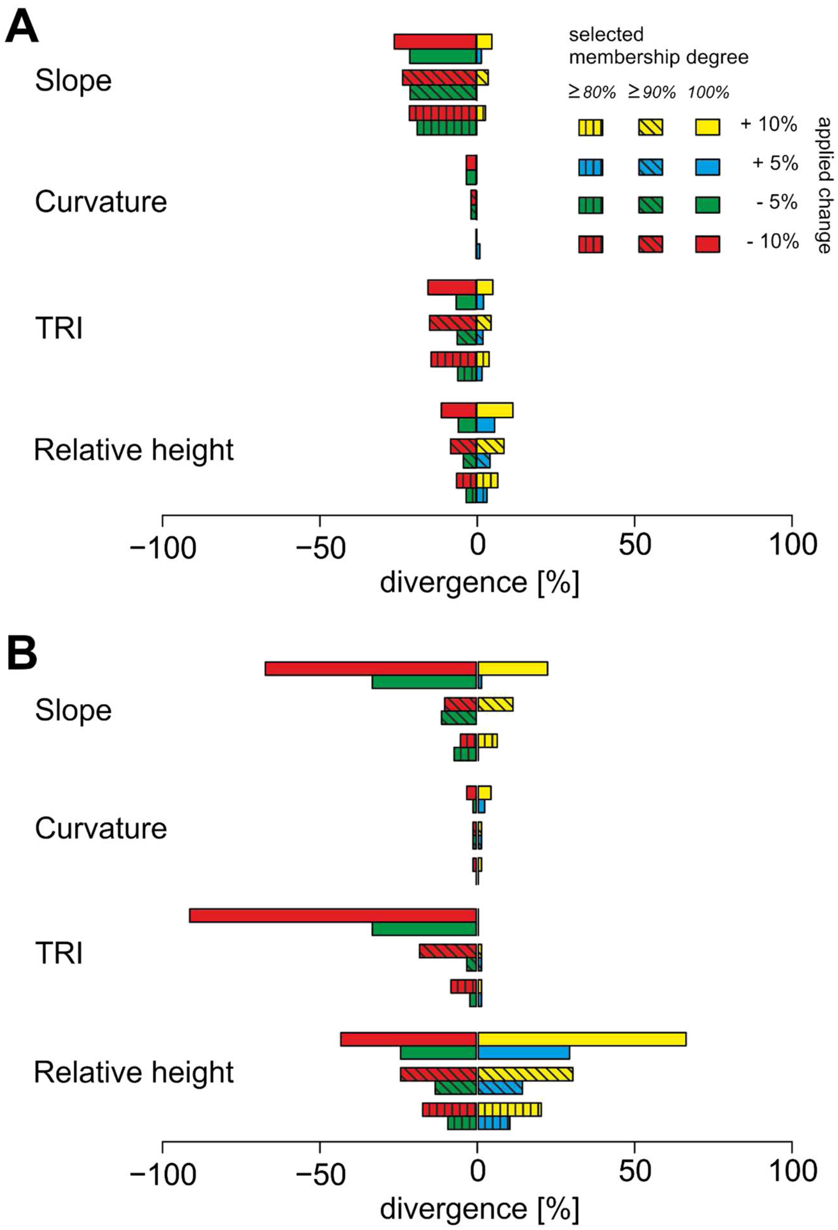

Figure 13. The two plots show the relative change of each single criterion after applying fuzzy logic algorithm (plot A), and of the final model result (plot B) by increasing or decreasing the 100% membership degree (MD) values for either 5 or 10%. Additionally to the resulting 100% MD, two further result ranges (≥80% and ≥ 90% MD) were extracted and analyzed (all dashed bars of the plots). See text for further details of the different results and patterns. This figure is available in colour online at wileyonlinelibrary.com/journal/espl

Sensitivity analysis of PAT

To test the sensitivity of the model, a one-at-a-time approach was applied on Nam Co area including 18.2×10^6 data points (Figure 2). In each step, the '100% membership degree' (100% MD) range of a single criterion was modified at a time to obtain the sensitivity of every single criterion. Two different data sets were extracted. The first one was selected directly after applying the fuzzy logic algorithm of each criterion (illustrated in Figure 4A as step 4) and the second one from the final model result (Figure 4A, step 5). Four different ranges of the '100% MD' value were applied by either increasing or decreasing the selection by 5 or 10%. The count of pixels (converted to area) classified as peneplains with a membership degree of ≥ 80%, ≥ 90%, and 100% were obtained from the model for each criterion and analyzed. Additionally, the deviation of the received counts in relation to the counts of the two different results have been calculated (see Table I) and plotted (Figure 13).

Figures 13A and 13B highlight that curvature is the least sensitive criterion in the PAT model while slope is the most sensitive criterion related to the decrease of the 100% MD value range. Slope and TRI are especially sensitive if lower values are set as zero in the fuzzy logic calculation (all values smaller than 0.5° by slope, and smaller than 5 m by TRI respectively; see Table I and Figure 13B). In case of slope, more than 30% of the used data points hold a value between 0.25° and 0.5° (Table I and Figure 13B). The maximum divergence of the resulting membership degree value is less than 30% by the range reduction of −10% (see Figure 13A). The increase of the 100% MD value of 10% induces a divergence of less than 15%. The uneven distribution of the divergence (higher sensitivity by decreasing the range) is reasonable by the previously applied best fit of the 100% MD range.

About 60% of the selected final data set plot between 3 and 5 m after the TRI modification but have no significant impact on the higher range (>80 m; see Table I).

Table I. Model results

Manipulated criteria		Range of the 100% MD value		Counts of the membership degree and percentage change					
				≥ 80%		≥ 90%		100%	
		Minimum	Maximum	Counts	Percent	Counts	Percent	Counts	Percent
Intermediary model result after applying fuzzy logic algorithm									
Slope	STD	0	10	11234169	—	10395390	—	9480056	—
	−10%	0.500	9.500	8814154	−21.5	7936830	−23.7	6980621	−26.4
	−5%	0.250	9.750	9100130	−19.0	8184330	−21.3	7452514	−21.4
	5%	0.000	10.500	11234169	0.0	10395390	0.0	9622687	1.5
	10%	0.000	11.000	11548226	2.8	10778047	3.7	9944334	4.9
Curvature	STD	−0.14	0.14	15646915	—	14525241	—	12503465	—
	−10%	−0.133	0.133	15646915	0.0	14291998	−1.6	12118837	−3.1
	−5%	−0.137	0.137	15646915	0.0	14291998	−1.6	12118837	−3.1
	5%	−0.144	0.144	15797095	1.0	14525241	0.0	12503465	0.0
	10%	−0.147	0.147	15797095	1.0	14525241	0.0	12503465	0.0
TRI	STD	1	80	11500146	—	11330509	—	11160323	—
	−10%	4.950	76.050	9836174	−14.5	9632816	−15.0	9427327	−15.5
	−5%	2.975	78.025	10823300	−5.9	10635948	−6.1	10449131	−6.4
	5%	0.000	82.950	11696410	1.7	11552723	2.0	11408942	2.2
	10%	0.000	86.900	11958124	4.0	11848837	4.6	11738408	5.2
Relative height	STD	100	600	10460775	—	9292722	−18.0	7854770	—
	−10%	125.000	575.000	9803773	−6.3	8528630	−8.2	6975653	−11.2
	−5%	112.500	587.500	10129616	−3.2	8907850	−4.1	7410646	−5.7
	5%	87.500	612.500	10809388	3.3	9693118	4.3	8308738	5.8
	10%	75.000	625.000	11171369	6.8	10106360	8.8	8777704	11.7
Result of the final model									
Original result	100%	—	—	2,271,529	—	1,114,005	—	75,429	—
Slope	−10%	0.500	9.500	2,154,920	−5	999,167	−10	24,539	−67
	−5%	0.250	9.750	2,123,697	−7	986,490	−11	50,509	−33
	5%	0.000	10.500	2,274,966	0	1,117,908	0	76,304	1
	10%	0.000	11.000	2,403,814	6	1,239,130	11	92,195	22
Curvature	−10%	−0.133	0.133	2,255,478	−1	1,099,009	−1	72,797	−3
	−5%	−0.137	0.137	2,264,885	0	1,107,863	−1	74,398	−1
	5%	−0.144	0.144	2,280,313	0	1,122,332	1	76,985	2
	10%	−0.147	0.147	2,286,906	1	1,128,505	1	78,286	4
TRI	−10%	4.950	76.050	2,086,307	−8	913,105	−18	6,549	−91
	−5%	2.975	78.025	2,234,514	−2	1,082,233	−3	50,645	−33
	5%	0.000	82.950	2,286,884	1	1,120,334	1	75,493	0
	10%	0.000	86.900	2,303,861	1	1,126,984	1	75,557	0
Relative height	−10%	125.000	575.000	1,883,483	−17	848,181	−24	43,226	−43
	−5%	112.500	587.500	2,068,089	−9	974,383	−13	56,996	−24
	5%	87.500	612.500	2,490,796	10	1,267,772	14	97,606	29
	10%	75.000	625.000	2,726,970	20	1,443,700	30	125,552	66

Note: the applied range of the 100% membership degree (100% MD) value for fuzzy logic algorithm, the resulting counts of pixel with a membership degree value of ≥ 80%, ≥ 90%, and 100%, and the relative change in percentage to the finally used values for PAT. The upper part of the table represents the intermediary result of each single criterion directly after applying the fuzzy logic algorithm in the model (Figure 4A illustrated in step 4). The first row of each criterion shows the analysis and results of the final used PAT. The lower part of the table shows the different applied ranges due to the 100% MD values and its finally results in the modified PAT (step 5 displayed in Figure 4A).

The criterion 'relative height' is more sensitive to the increase of the 100% MD value range in the fuzzy logic algorithm. Compared to the applied change for the final model result, the investigated sensitivity of the criterion directly after applying fuzzy logic is remarkably less sensitive (Figure 13B). Relative height is very sensitive for both, decreasing or increasing the 100% MD value range. Therefore this criterion has a high impact on the final result of the PAT model. Relative height can be justified if for example nearly leveled peneplains or extraordinary high elevated peneplains (rh > 600 m) are desired.

The extracted pixel counts with membership degree values ≥ 80% and ≥ 90% of the PAT have a similar sensitivity directly after applying the fuzzy logic algorithm but are less sensitive in the final PAT model result compared to the selected 100% MD value. Consequently, the sensitivity declines with the enlargement of the final membership degree selection at the end of the PAT model.

Discussion and Conclusions

It was demonstrated that the peneplains identified by the newly developed PAT method in the central Tibetan Plateau correspond to our field observations as shown in Figure 10. The new method confirms already described peneplains in other areas such as the Massif Central (France), the central Andes, the Appalachian Mountains, and in the southern part of New Zealand. PAT was not able to identify the intensely discussed peneplains in the Pyrenees. While PAT exclusively focuses on the geometry of the landscape, the peneplain-like geomorphologic domains in the Pyrenees which are controversially discussed in the literature were described fully from a genetic point of view (e.g. Babault *et al.*, 2005; Gunnell *et al.*, 2009).

The thresholds for the three criteria slope, curvature, and TRI determined in our study are used universally for the identification of peneplains. The 'relative height' is based on the calculated drainage system and it is potentially adjustable to calculate lower elevated peneplains or peneplains with a certain spectrum of relative elevation. Furthermore any anomalies as for example interfering minor depressions of the topography can be computed in DEMs (e.g. Nobre *et al*., 2011, and references cited therein). Nevertheless many models were developed to simulate hydrological processes using DEMs (e.g. Tarboton, 1997; Curkendall *et al*., 2003; Nobre *et al*., 2011) and these tools provide different ways to suppress disturbing interference (e.g. O'Callaghan and Mark, 1984; Garbrecht and Martz, 1997; Jones, 2002; Nobre *et al*., 2011).

Compared to these hydrological relevant models our model operates at a considerably larger scale with a minimum area of around 2000 km^2. Cell interferences at high resolution have no significant impact on our method to calculate the 'relative height' and to delineate the peneplains. However, the parameter 'relative height' is sensitive and can be tuned in several cases, according to the depth of modern incision, the typical relief of the region, and of course the definition of the minimum height of peneplains. There are two possibilities for the proper setting of relative height. Firstly, the drainage network can be set to be coarse or fine which results in a smooth or undulating base level, respectively. Using a fine drainage network (considering small catchments), the calculated erosional base level 'follows' the topography and, thus, the relative height remains always small. Using a coarse drainage network (only the well developed branches of the drainage system), the relative height increases and the elevated surfaces become easier to identify (see also Figure 7). The second possibility, i.e. adjusting the 'relative height' criteria to the typical local relief (to the altitude of peneplain relatively to the regional erosion level), is to set the 100% acceptance of the fuzzy logic. The most robust acceptance value that was determined in central Tibet is the range of 100 to 600 m and this range works well in several other settings worldwide. However, when the peneplain experienced only minor uplift, the acceptance range should be reduced. Our applications of the PAT method in different areas worldwide show that it is possible to set the thresholds in such a way, that the regional characteristics are accounted for and the peneplains are successfully identified.

We conclude that it is possible to set up a representative criteria system to identify peneplains using solely morphometric parameters derived from digital elevation data. It appears that only a coincidence of multiple criteria can lead to a successful delineation of geomorphological features, which can be classified as peneplains.

The global availability of the homogeneous DEM allows the application of this approach on the regional scale independently of the geographical location. The peneplains identified by the fuzzy logic model in various geological settings appear to be in a good accordance with the findings described in the literature. This strongly corroborates our assumption that peneplains can be characterized in a uniform way regardless of their age, elevation or geographical location. However, this approach can lead to certain misidentification with peneplains described in the literature in cases when purely genetic criteria were employed for their identification. A favorable side effect of modeling with PAT is the additional highlighting of extensive intermontane basins (see Figure 11A). The PAT method was shown to be a robust new approach to identify and validate peneplains. An unbiased definition and delineation of peneplains is a fundamental step that allows for further systematic investigation of peneplains with respect to their genesis, age, and geological structure at the regional scale. The proposed method can thus contribute to better understanding of this intensely discussed geomorphological phenomenon.

Acknowledgements—The authors thank Balázs Székely (Budapest) for a helpful key discussion and Raimon Tolosana-Delgado (HZDR, Germany) for his crucial comments in statistical issues. This research was funded by the German Research Foundation (DFG) in the framework of the priority program 1372 entitled Tibetan Plateau: Formation – Climate Ecosystem (grant DU 373/5). The authors thank METI and NASA for providing the digital elevation model (SRTM) and CIAT for providing processed SRTM Data Version 4.1 (http://srtm.jrc.ec.europa.eu/). Associate Editor Josh Roering and three further anonymous reviewers provided helpful and constructive reviews. Sincere thanks are due to Sinéad O'Keeffe for linguistic improvement of the manuscript.

References

Aalto KR. 2006. The Klamath Peneplain: A Review of J. S. Diller's Classic Erosion Surface. Geological Studies in the Klamath Mountains Province, California and Oregon. A Volume in Honor of William P. Irwin. The Geological Society of America Special Papers 410. The Geological Society of America: Boulder, CO; 451–463.

Adams J. 1980. Contemporary uplift and erosion of the Southern Alps, New Zealand. *Geological Society of America Bulletin* **91**(1 Part II): 1–114. DOI: B25974.1/GSAB-P2-91-1

Allmendinger RW, González G. 2010. Invited review paper: Neogene to Quaternary tectonics of the coastal Cordillera, northern Chile. *Tectonophysics* **495**(1): 93–110. DOI: 10.1016/j.tecto.2009.04.019

Anderson FM. 1902. The physiographic features of the Klamath Mountains. *The Journal of Geology* **10**(2): 144–159.

Babault J, Bonnet S, Driessche JVD, Crave A. 2007. High elevation of low-relief surfaces in mountain belts: does it equate to post-orogenic surface uplift? *Terra Nova* **19**(4): 272–277. DOI: 10.1111/j.1365-3121.2007.00746.x

Babault J, van Den Driessche J, Bonnet S, Castelltort S, Crave A. 2005. Origin of the highly elevated Pyrenean peneplain. *Tectonics* **24**(2): 1–19. DOI: 10.1029/2004TC001697

Baulig H. 1957. Peneplains and pediplains. *Geological Society of America Bulletin* **68**(7): 913–930. DOI: B25974.1/0016-7606(1957)68[913:PAP]2.0.CO;2

Bethune PF. 1948. Geomorphic studies in the Appalachians of Pennsylvania. *American Journal of Science* **246**(1): 1–22. DOI: 10.2475/ajs.246.1.1

Biacino L, Gerla G. 2002. Fuzzy logic, continuity and effectiveness. *Archive for Mathematical Logic* **41**(7): 643–667. DOI: 10.1007/s001530100128

Burrough PA, McDonell RA. 1998. Principles of Geographical Information Systems. Oxford University Press: New York; 190.

Campbell KE, Frailey CD, Romero-Pittman L. 2006. The Pan-Amazonian Ucayali Peneplain, late Neogene sedimentation in Amazonia, and the birth of the modern Amazon River system. *Palaeogeography, Palaeoclimatology, Palaeoecology* **239**(1–2): 166–219. DOI: 10.1016/j.palaeo.2006.01.020

Clark MK, Schoenbohm LM, Royden LH, Whipple KX, Burchfiel BC, Zhang X, Tang W, Wang E, Chen L. 2004. Surface uplift, tectonics, and erosion of eastern Tibet from large-scale drainage patterns. *Tectonics* **23**(1): 1–20. DOI: 10.1029/2002TC001402

Cole WS. 1934. Identification of erosion surfaces in eastern and southern Ohio. *The Journal of Geology* **42**(3): 285–294.

Coltorti M, Dramis F, Ollier CD. 2007. Planation surfaces in northern Ethiopia. *Geomorphology* **89**(3–4): 287–296. DOI: 10.1016/j.geomorph.2006.12.007

Coombs DS, White AJR, Hamilton D, Couper RA. 1960. Age relations of the Dunedin volcanic complex and some paleogeographic implications—Part II. *New Zealand Journal of Geology and Geophysics* **3**(4): 572–579. DOI: 10.1080/00288306.1960.10420145

Cui Z, Gao Q, Liu G, Pan B, Chen H. 1997. The initial elevation of palaeokarst and planation surfaces on Tibet Plateau. *Chinese Science Bulletin* **42**(11): 934–939. DOI: 10.1007/BF02882552

Curkendall DW, Fielding EJ, Cheng TH, Pohl JM. 2003. A computational-grid based system for continental drainage network extraction using SRTM digital elevation models. *Proceeding, Parallel Processing Workshops International Conference*; 181–190. DOI: 10.1109/ICPPW.2003.1240369

Davis WM. 1899. The geographical cycle. *Geographical Journal* **14**(5): 481–504.

Davis WM. 1902. Baselevel, grade and peneplain. *The Journal of Geology* **10**(1): 77–111.

DeSitter LU. 1952. Pliocene uplift of Tertiary mountain chains. *American Journal of Science* **250**(4): 297–307. DOI. 10.2475/ajs.250.4.297

Dixey F. 1939. The Early Cretaceous valley-floor pene-plain of the Lake Nyasa region and its relation to tertiary rift structures. *Quarterly Journal of the Geological Society* **95**(1–4): 75–108. DOI: 10.1144/GSL.JGS.1939.065.01-04.05

Fairbridge RW, Finkl Jr CW. 1980. Cratonic erosional unconformities and peneplains. *The Journal of Geology* **88**(1): 69–86.

Farr T, Kobrick M. 2001. The shuttle radar topography mission. *Eos, Transactions American Geophysical Union* **82**: 47. DOI: 10.1029/EO081i048p00583

Fielding E, Isacks B, Barazangi M, Duncan C. 1994. How flat is Tibet? *Geology* **22**(2): 163–167. DOI. B25974./0091-7613(1994)0220163:HFIT2.3.CO;2

Fridley HM, Nölting Jr JP. 1931. Peneplains of the Appalachian Plateau. *The Journal of Geology* **39**(8): 749–755.

Galli-Olivier C. 1967. Pediplain in northern Chile and the Andean uplift. *Science* **158**(3801): 653–655. DOI: 10.1126/science.158.3801.653

Garbrecht J, Martz LW. 1997. The assignment of drainage direction over flat surfaces in raster digital elevation models. *Journal of Hydrology* **193**(1–4): 204–213. DOI: 10.1016/S0022-1694(96)03138-1

Garcia-Castellanos D, Cloetingh S, van Balen R. 2000. Modelling the Middle Pleistocene uplift in the Ardennes-Rhenish Massif: thermo-mechanical weakening under the Eifel? *Global and Planetary Change* **27**(1): 39–52. DOI: 10.1016/S0921-8181(01)00058-3

Gjessing J. 1967. Norway's paleic surface. *Norsk Geografisk Tidsskrift – Norwegian Journal of Geography* **21**(2): 69–132. DOI: 10.1080/00291956708621854

Granet M, Wilson M, Achauer U. 1995. Imaging a mantle plume beneath the French Massif Central. *Earth and Planetary Science Letters* **136**(3): 281–296. DOI. 10.1016/0012-821X(95)00174-B

Gunnell Y, Calvet M, Brichau S, Carter A, Aguilar JP, Zeyen H. 2009. Low long-term erosion rates in high-energy mountain belts: insights from thermo-and biochronology in the eastern Pyrenees. *Earth and Planetary Science Letters* **278**(3–4): 208–218. DOI: 10.1016/j.epsl.2008.12.004

Hack JT. 1975. Dynamic equilibrium and landscape evolution. In Theories of Landform Evolution, Melhorn WN, Flemal RC (eds). Allen & Unwin: Crows Nest; 87–102.

Haider VL, Dunkl I, von Eynatten H, Ding L, Frei D, Zhang L. 2013. Cretaceous to Cenozoic evolution of the northern Lhasa Terrane and the Early Paleogene development of peneplains at Nam Co, Tibetan Plateau. *Journal of Asian Earth Sciences* **70–71**: 79–98. DOI: 10.1016/j.jseaes.2013.03.005

Hall AM, Ebert K, Kleman J, Nesje A, Ottesen D. 2013. Selective glacial erosion on the Norwegian passive margin. *Geology* **41**(12): 1203–1206. DOI: 10.1130/G34806.1

Hetzel R, Dunkl I, Haider V, Strobl M, von Eynatten H, Ding L, Frei D. 2011. Peneplain formation in southern Tibet predates the India-Asia collision and plateau uplift. *Geology* **39**(10): 983–986. DOI: 10.1130/G32069.1

Hoke GD, Garzione CN. 2008. Paleosurfaces, paleoelevation, and the mechanisms for the late Miocene topographic development of the Altiplano plateau. *Earth and Planetary Science Letters* **271**(1–4): 192–201. DOI: 10.1016/j.epsl.2008.04.008

Hoke GD, Isacks BL, Jordan TE, Blanco N, Tomlinson AJ, Ramezani J. 2007. Geomorphic evidence for post-10 Ma uplift of the western flank of the central Andes 18 30′–22 S. *Tectonics* **26**(5): 1–17. DOI: 10.1029/2006TC002082

Hurst MD, Mudd SM, Yoo K, Attal M, Walcott R. 2013. Influence of lithology on hillslope morphology and response to tectonic forcing in the northern Sierra Nevada of California. *Journal of Geophysical Research, Earth Surface* **118**(2): 832–851. DOI: 10.1002/jgrf.20049

Jackson J, Norris R, Youngson J. 1996. The structural evolution of active fault and fold systems in central Otago, New Zealand: evidence revealed by drainage patterns. *Journal of Structural Geology* **18**(2): 217–234. DOI: 10.1016/S0191-8141(96)80046-0

Jackson J, Ritz JF, Siame L, Raisbeck G, Yiou F, Norris R, Youngson J, Bennett E. 2002. Fault growth and landscape development rates in Otago, New Zealand, using *in situ* cosmogenic ^{10}Be. *Earth and Planetary Science Letters* **195**(3): 185–193. DOI: 10.1016/S0012-821X(01)00583-0

Jarvis A, Reuter HI, Nelson A, Guevara E. 2008. Hole-filled SRTM for the globe Version 4. Available from the CGIARCSI SRTM 90m Database. http://srtm csi cgiar org 2007 [15 June 2012].

Jixiang Y, Juntao X, Chengjie L, Huan L. 1988. The Tibetan plateau: regional stratigraphic context and previous work. *Philosophical Transactions of the Royal Society of London. Series A. Mathematical and Physical Sciences* **327**(1594): 5–52. DOI: 10.1098/rsta.1988.0121

Jones R. 2002. Algorithms for using a DEM for mapping catchment areas of stream sediment samples. *Computers & Geosciences* **28**(9): 1051–1060. DOI: 10.1016/S0098-3004(02)00022-5

Jordan TE, Zeitler P, Ramos V, Gleadow AJW. 1989. Thermochronometric data on the development of the basement peneplain in the Sierras Pampeanas, Argentina. *Journal of South American Earth Sciences* **2**(3): 207–222. DOI: 10.1016/0895-9811(89)90030-8

Kennan L, Lamb SH, Hoke L. 1997. High-altitude palaeosurfaces in the Bolivian Andes: evidence for late Cenozoic surface uplift. *Special Publication – Geological Society of London* **120**: 307–323. DOI: 10.1144/GSL.SP.1997.120.01.20

Kummel B. 1948. Geological reconnaissance of the Contamana region, Peru. *Geological Society of America Bulletin* **59**(12): 1217–1266. DOI: 10.1130/0016-7606(1948)59[1217:GROTCR]2.0.CO;2

Lamb S, Hoke L, Kennan L, Dewey J. 1996. Cenozoic evolution of the central Andes in Bolivia and northern Chile. *Special Publication – Geological Society of London* **121**: 237–264. DOI: 10.1144/GSL.SP.1997.121.01.10

Landis CA, Campbell HJ, Begg JG, Mildenhall DC, Paterson AM, Trewick SA. 2008. The Waipounamu erosion surface: questioning the antiquity of the New Zealand land surface and terrestrial fauna and flora. *Geological Magazine* **145**(2): 173–197. DOI: 10.1017/S0016756807004268

Leeder MR, Smith AB, Jixiang Y. 1988. Sedimentology, palaeoecology and palaeoenvironmental evolution of the 1985 Lhasa to Golmud Geotraverse. *Philosophical Transactions of the Royal Society of London. Series A. Mathematical and Physical Sciences* **327**(1594): 107–143. DOI: 10.1098/rsta.1988.0123

Leier AL, DeCelles P, Kapp P, Ding L. 2007. The Takena Formation of the Lhasa terrane, southern Tibet. The record of a Late Cretaceous retroarc foreland basin. *Geological Society of America Bulletin* **119**: 31–48. DOI: 10.1130/B25974.1119

LeMasurier WE, Landis CA. 1996. Mantle-plume activity recorded by low-relief erosion surfaces in West Antarctica and New Zealand. *Geological Society of America Bulletin* **108**(11): 1450–1466. DOI: 10.1130/0016-7606(1996)108<1450:MPARBL>2.3.CO;2

Lidmar-Bergström K. 1999. Uplift histories revealed by landforms of the Scandinavian domes. *Special Publications – Geological Society of London* **162**(1): 85–91. DOI: 10.1144/GSL.SP.1999.162.01.07

Lindgren W, Livingston DC. 1918. The Idaho peneplain (discussion). *Economic Geology* **13**(6): 486–492. DOI: 10.2113/gsecongeo.13.6.486

Liu-Zeng J, Tapponnier P, Gaudemer Y, Ding L. 2008. Quantifying landscape differences across the Tibetan plateau. Implications for topographic relief evolution. *Journal of Geophysical Research* **113**(F4): F04018. DOI: 10.1029/2007JF000897

Markley M, Norris RJ. 1999. Structure and neotectonics of the Blackstone Hill Antiform, Central Otago, New Zealand. *New Zealand Journal of Geology and Geophysics* **42**(2): 205–218. DOI: 10.1080/00288306.1999.9514840

McMillan ME, Heller PL, Wing SL. 2006. History and causes of post-Laramide relief in the Rocky Mountain orogenic plateau. *Geological Society of America Bulletin* **118**(3–4): 393–405. DOI: 10.1130/B25712.1

Métivier F, Gaudemer Y, Tapponnier P, Meyer B. 1998. Northeastward growth of the Tibet plateau deduced from balanced reconstruction of two depositional areas. The Qaidam and Hexi Corridor basins, China. *Tectonics* **17**(6): 823–842. DOI: 10.1029/98TC02764

Mulcahy MJ, Churchward HM, Dimmock GM. 1972. Landforms and soils on an uplifted peneplain in the Darling Range Western Australia. *Soil Research* **10**(1): 1–14. DOI: 10.1071/SR9720001

Muñoz V, Hérail G, Farías M. 2008. Nature of a topographic height in the Tarapacá pediplain, northern Chile. *Proceedings, 7th International Symposium on Andean Geodynamics (ISAG 2008, Nice). Extended Abstracts*; 365–368.

Nobre AD, Cuartas LA, Hodnett M, Rennó CD, Rodrigues G, Silveira A, Waterloo M, Saleska S. 2011. Height above the nearest drainage – a hydrologically relevant new terrain model. *Journal of Hydrology* **404** (1): 13–29. DOI: 10.1016/j.jhydrol.2011.03.051

O'Callaghan JF, Mark DM, 1984. The extraction of drainage networks from digital elevation data. *Computer Vision, Graphics, and Image Processing* **28**(3): 323–344. DOI: 10.1016/S0734-189X (84)80011-0

Olaya V. 2009. Basic land-surface parameters. *Developments in Soil Science* **33**: 141–169. DOI: 10.1016/S0166-2481(08)00006-8

Pan G, Ding J, Yao D, Wang L. 2004. Geological Map of Qinghai-Xizang (Tibet) Plateau and Adjacent Areas (1. 1,500,000). Chengdu Cartographic Publishing House: Chengdu.

Patriat P, Achache J. 1984. India-Eurasia collision chronology has implications for crustal shortening and driving mechanism of plates. *Nature* **311**: 615–621. DOI: 10.1038/311615a0

Peckham SD, Hengl T, Evans J, Wilson JP, Gould M. 2011. Profile, plan and streamline curvature: a simple derivation and applications. *Geomorphometry* 27–30.

Penck W. 1924. Die morphologische Analyse. Ein Kapital der physikalischen Geologie. Engelhorn: Stuttgart; 283.

Pitman WC, Golovchenko X. 1991. The effect of sea level changes on the morphology of mountain belts. *Journal of Geophysical Research* **96**(B4): 6879–6891. DOI: 10.1029/91JB00250

Reuter HI, Nelson A, Jarvis A. 2007. An evaluation of void-filling interpolation methods for SRTM data. *International Journal of Geographical Information Science* **21**(9): 983–1008. DOI: 10.1080/13658810601169899

Riley SJ, DeGloria SD, Elliot R. 1999. A terrain ruggedness index that quantifies topographic heterogeneity. *Intermountain Journal of Sciences* **5**(1–4): 23–27.

Roering JJ, Kirchner JW, Dietrich WE. 2005. Characterizing structural and lithologic controls on deep-seated landsliding: Implications for topographic relief and landscape evolution in the Oregon Coast Range, USA. *Geological Society of America Bulletin* **117**(5–6): 654–668. DOI: 10.1130/B25567.1

Santos ES. 1970. Fuzzy algorithms. *Information and Control* **17**(4): 326–339. DOI: 10.1016/S0019-9958(70)80032-8

Schildgen TF, Ehlers TA, Whipp DM, van Soest MC, Whipple KX, Hodges KV. 2009. Quantifying canyon incision and Andean Plateau surface uplift, southwest Peru: a thermochronometer and numerical modeling approach. *Journal of Geophysical Research* **114**(F04014): 1–22. DOI: 10.1029/2009JF001305

Sevon WD, Potter N, Crowl GH. 1983. Appalachian peneplains: an historical review. *Earth Sciences History* **2**(2): 156–164.

Sheth HC. 2007. Plume-related regional prevolcanic uplift in the Deccan Traps: absence of evidence, evidence of absence. *Geological Society of America Special Papers* **430**: 785–813. DOI: 10.1130/2007.2430(36)

Simon-Coinçon R, Thiry M, Schmitt JM. 1997. Variety and relationships of weathering features along the early Tertiary palaeosurface in the southwestern French Massif Central and the nearby Aquitaine Basin. *Palaeogeography, Palaeoclimatology, Palaeoecology* **129**(1): 51–79. DOI: 10.1016/S0031-0182(96)00122-8

Sinclair HD, Gibson M, Lynn G, Stuart F. 2009. The evidence for a Pyrenean resurrection: a response to Babault *et al.* (2008). *Basin Research* **21**(1): 143–145. DOI: 10.1111/j.1365-2117.2008.00391.x

Smith GH. 1935. The relative relief of Ohio. *Geographical Review* **25** (2): 272–284.

Steer P, Huismans RS, Valla PG, Gac S, Herman F. 2012. Bimodal Plio-Quaternary glacial erosion of fjords and low-relief surfaces in Scandinavia. *Nature Geoscience* **5**(9): 635–639. DOI: 10.1038/ngeo1549

Stirling MW. 1991. Peneplain modification in an alpine environment of Central Otago, New Zealand. *New Zealand Journal of Geology and Geophysics* **34**(2): 195–201. DOI: 10.1080/00288306.1991.9514457

Stose GW. 1940. Age of the Schooley peneplain. *American Journal of Science* **238**(7): 461–476. DOI: 10.2475/ajs.238.7.461

Strobl M, Hetzel R, Ding L, Zhang L, Hampel A. 2010. Preservation of a large-scale bedrock peneplain suggests long-term landscape stability in southern Tibet. *Zeitschrift für Geomorphologie* **54**(4): 453–466. DOI: 10.1127/0372-8854/2010/0054-0023

Strobl M, Hetzel R, Niedermann S, Ding L, Zhang L 2012. Landscape evolution of a bedrock peneplain on the southern Tibetan Plateau revealed by in situ-produced cosmogenic ^{10}Be and ^{21}Ne. *Geomorphology* **153–154**: 192–204. DOI: 10.1016/j.geomorph.2012.02.024

Strøm KM. 1948. The geomorphology of Norway. *The Geographical Journal* **112**(1/3): 19–23.

Sturkell E, Lindström M. 2004. The target peneplain of the Lockne impact. *Meteoritics & Planetary Science* **39**(10): 1721–1731. DOI: 10.1111/j.1945-5100.2004.tb00068.x

Tarboton DG. 1997. A new method for the determination of flow directions and upslope areas in grid digital elevation models. *Water Resources Research* **33**(2): 309–319. DOI: 10.1029/96WR03137

Tarboton DG, Bras RL, Rodriguez-Iturbe I. 1991. On the extraction of channel networks from digital elevation data. *Hydrological Processes* **5**(1): 81–100. DOI: 10.1002/hyp.3360050107

van der Beek P, van Melle J, Guillot S, Pêcher A, Reiners PW, Nicolescu S, Latif M. 2009. Eocene Tibetan plateau remnants preserved in the northwest Himalaya. *Nature Geoscience* **2**(5): 364–368. DOI: 10.1038/ngeo503

White WB. 2009. The evolution of Appalachian fluviokarst: competition between stream erosion, cave development, surface denudation, and tectonic uplift. *Journal of Cave and Karst Studies* **71**(3): 159–167. DOI: 10.4311/jcks2008es0046

Willis B. 1933. The peneplains of East Africa. *The Geographical Journal* **82**(4): 383–384.

Wörner G, Uhlig D, Kohler I, Seyfried H. 2002. Evolution of the western Andean Escarpment at 18°S (N. Chile) during the last 25 Ma: uplift, erosion and collapse through time. *Tectonophysics* **345**(1–4): 183–198. DOI: 10.1016/S0040-1951(01)00212-8

Zadeh LA. 1968. Fuzzy algorithms. *Information and Control* **12**(2): 94–102.

Zevenbergen LW, Thorne CR. 1987. Quantitative analysis of land surface topography. *Earth Surface Processes and Landforms* **12**(1): 47–56. DOI: 10.1002/esp.3290120107

Zeyen H, Novak O, Landes M, Prodehl C, Driad L, Hirn A. 1997. Refraction-seismic investigations of the northern Massif Central (France). *Tectonophysics* **275**(1): 99–117. DOI: 10.1016/S0040-1951(97)00017-6

